High resolution polarization-independent high-birefringence fiber loop mirror sensor

Daniel Leandro,* Mikel Bravo and Manuel Lopez-Amo

Universidad Pública de Navarra, Campus Arrosadía s/n, 31006 Pamplona, Spain
**daniel.leandro@unavarra.es*

Abstract: In this work, two all polarization-maintaining (PM) high-birefringence (Hi-Bi) fiber loop mirrors (FLM) which are immune to external polarization perturbations are validated both theoretically and experimentally. Simplified and stable versions of classical FLMs were attained using a PM-coupler and by fusing the different Hi-Bi fiber sections with an adequate rotation angle between them. Since the polarization states are fixed along the whole fiber loop, no polarization controllers are needed. This simplifies the operation and increases the stability of the systems, which were also validated as ultra-high resolution sensors, experimentally obtaining a resolution of $6.2 \cdot 10^{-4}$ °C without averaging.

OCIS codes: (060.2420) Fibers, polarization-maintaining; (060.2370) Fiber optics sensors.

References and links

1. D. Mortimore, "Fiber loop reflectors," J. Lightwave Technol. **6**(7), 1217–1224 (1988).
2. Y. Liu, B. Liu, X. Feng, W. Zhang, G. Zhou, S. Yuan, G. Kai, and X. Dong, "High-birefringence fiber loop mirrors and their applications as sensors," Appl. Opt. **44**(12), 2382–2390 (2005).
3. S. Li, K. S. Chiang, and W. A. Gambling, "Gain flattening of an erbium doped fiber amplifier using a High-Birefringence fiber loop mirror," IEEE Photonics Technol. Lett. **13**(9), 942–944 (2001).
4. A. M. R. Pinto, M. Bravo, M. Fernandez-Vallejo, M. Lopez-Amo, J. Kobelke, and K. Schuster, "Suspended-core fiber Sagnac combined dual-random mirror Raman fiber laser," Opt. Express **19**(12), 11906–11915 (2011).
5. S. Chung, B. A. Yu, and B. Lee, "Phase response design of a polarization-maintaining fiber loop mirror for dispersion compensation," IEEE Photonics Technol. Lett. **15**(5), 715–717 (2003).
6. O. Frazão, J. M. Baptista, and J. L. Santos, "Recent advances in high-birefringence fiber loop mirror sensors," Sensors (Basel Switzerland) **7**(11), 2970–2983 (2007).
7. D. Barrera, J. Villatoro, V. P. Finazzi, G. A. Cardenas-Sevilla, V. P. Minkovich, S. Sales, and V. Pruneri, "Low-loss photonic crystal fiber interferometers for sensor networks," J. Lightwave Technol. **28**(24), 3542–3547 (2010).
8. M. Bravo, M. Fernández-Vallejo, M. Echapare, M. López-Amo, J. Kobelke, and K. Schuster, "Multiplexing of six micro-displacement suspended-core Sagnac interferometer sensors with a Raman-Erbium fiber laser," Opt. Express **21**(3), 2971–2977 (2013).
9. G. A. Cárdenas-Sevilla, V. Finazzi, J. Villatoro, and V. Pruneri, "Photonic crystal fiber sensor array based on modes overlapping," Opt. Express **19**(8), 7596–7602 (2011).
10. H. Y. Fu, A. C. L. Wong, P. A. Childs, H. Y. Tam, Y. B. Liao, C. Lu, and P. K. A. Wai, "Multiplexing of polarization-maintaining photonic crystal fiber based Sagnac interferometric sensors," Opt. Express **17**(21), 18501–18512 (2009).
11. D. Leandro, M. Bravo, A. Ortigosa, and M. Lopez-Amo, "Real-Time FFT Analysis for Interferometric Sensors Multiplexing," J. Lightwave Technol. **33**(2), 354–360 (2015).

1. Introduction

High-birefringence (Hi-Bi) fibers have attracted great interest the last years due to their capability to preserve the polarization state of light. If the light launched into the fiber is aligned with one of the birefringent axes, the polarization state of light will be preserved, albeit the fiber is bent. These fibers are also known as polarization-maintaining (PM) fibers and have many applications in fiber lasers, non-linear optics, optical sensing and telecommunications. Hi-Bi fibers are often inserted in interferometers in order to exploit the phase shift between the polarization axes. One of these topologies is the fiber loop mirror

#249263 Received 1 Sep 2015; revised 28 Oct 2015; accepted 16 Nov 2015; published 19 Nov 2015

(FLM) [1] which has been studied for applications such as optical filtering [2], fiber amplification [3], fiber lasers [4], dispersion compensation [5] and optical sensing [6].

However, in the sensing field, this technology has some serious weaknesses that must be addressed in order to compete with other sensing technologies such as fiber Bragg gratings. The first one is its poor multiplexing capability. A few works have been published in this respect [7–11], being of special interest the fast Fourier transform (FFT) analysis used in [7,11]. Typically, when several interferometric sensors are multiplexed, the interference resulting is a combination of sinusoidal functions which make the classical interference valleys tracking technique non-feasible. In this regard, the FFT analysis allows isolating each characteristic frequency of the interferometers multiplexed, having the sensing information included in the FFT phase. Another critical weakness of FLMs is its high dependence on polarization changes induced in the single mode fiber (SMF) sections. This is because the polarization of light that propagates in SMF fiber gradually changes in an uncontrolled (and wavelength-dependent) manner. This implies that a polarization controller must be present inside the loop of the FLM, and needs to be frequently adjusted, especially if the FLM itself is exposed to external perturbations such as vibrations. That is a restraint for its practical application since a change in the SMF of the loop can vary the reading of the sensor.

In this work, to address the mentioned limitations, two all-PM fiber loop mirrors are studied both theoretically and experimentally. In the first setup, the two ports of a PM-coupler are fused together with a fixed angle to obtain a simplified version of a simple FLM (without dependence on external perturbations on the polarization). A second setup is proposed where an all-silica HiBi fiber is included into the loop and measured as strain sensor. This is possible due to a precise control of the rotation angles during the fusion between fibers. Finally, these schemes are validated as ultra-high resolution sensors using the FFT analysis, obtaining independent temperature and strain readings with temperature errors under $6.2 \cdot 10^{-4}$ °C.

2. Operating principle

2.1 Two-section all-PM Hi-Bi FLM

The transfer function of a simple Hi-Bi FLM, formed by inserting a Hi-Bi fiber section between the output ports of a single-mode-fiber optical coupler, is as follows [2]:

$$T = \left[\sin(\theta_c) \cos\left((\pi l \lambda_0 / L_B \lambda) + \Delta\phi \right) \right]^2 \tag{1}$$

Where l represents the length of the Hi-Bi fiber, L_B the beat length, λ the wavelength and θ_c denotes the difference between the rotation angles of the polarization states at the ports of the coupler. On the other hand $\Delta\phi$ symbolizes the phase shift caused by changes in the birefringence of the fiber due to temperature or strain variations. As mentioned beforehand, one of the main limitations of Hi-Bi FLMs is the polarization change induced in the single mode fiber by external perturbations which considerably limits its practical usage. Thus, the FLM should be kept stable; otherwise a polarization controller (PC) placed into the loop has to be frequently adjusted. As a result, the PC is essential in every Hi-Bi FLM formed by a SMF-optical coupler. To eliminate this dependence, using a PM optical coupler could be considered a straightforward solution; however the ports of the PM-coupler themselves are made of Hi-Bi fiber. Consequently, the fiber loop would in fact be formed by two different sections of Hi-Bi fiber as depicted in Fig. 1(a). In that case, Eq. (1) is no longer valid and a more complex expression have to be used. This two-section model was initially reported in [2] for the design of optical filters, where n identifies the n-th HiBi section of the loop:

$$T = [\cos(\beta_1 + \beta_2)\cos(\theta)\sin(\theta_C) + \cos(\beta_1 - \beta_2)\sin(\theta)\cos(\theta_C)]^2 \; ; \quad \beta_n = \frac{\pi l_n \lambda_0}{L_{Bn} \lambda} + \Delta\phi_n \tag{2}$$

It is worth noting that using a fused PM optical coupler implies that the angle θ_c cannot be modified and it is fixed at $\theta_c = 0$. Accordingly, the optical interference generated by the

#249263 Received 1 Sep 2015; revised 28 Oct 2015; accepted 16 Nov 2015; published 19 Nov 2015

structure will depend only on the rotation angle between the fibers θ and their lengths. With the aim of maximizing the amplitude of the interference, the fiber sections are fused with a rotation offset of $\theta = 90°$ for the experimental verification. As a result, the transfer function of a polarization independent Hi-Bi FLM can be derived from Eq. (2) obtaining:

$$T = \left[\cos\left(\beta_1 - \beta_2\right)\right]^2 \tag{3}$$

That is a simplified version of the transfer function of a simple Hi-Bi FLM [Eq. (1)] with a Hi-Bi fiber length (l_1-l_2) but with no dependence on the polarization states change θ_c along the fiber. Since every rotation angle is fixed, no polarization controllers have to be tuned, easing the operation of the system and improving its performance. This also implies that it is virtually immune to external variations in the polarization, increasing its reliability as sensor.

In order to be validated, the system was measured experimentally. A 50:50 PM fused coupler fabricated with fiber type Panda SM15-PS-U25A with a measured beat length of 3.98 mm was used in the experiment. The output ports of the coupler were 0.625 and 1.125 m long respectively and were fused together with a rotation angle between them θ = 90°. The angle was fixed by the fusion splicer Fujikura FSM 100P, which allows a rotation angle control between fibers of 0.01°. The interference measured can be seen in Fig. 1(b). In addition, a simulation of the system based on Eq. (2) was carried out, which matches the experimental results. Taking into account that the distance between dips of the interference spectrum is given by: $\Delta\lambda = \lambda \cdot L_B/l$; the measured spectrum corresponds to the interference generated by a simple FLM with a Hi-Bi fiber of length $l = \lambda\, L_B/\Delta\lambda \approx 0.5$ m = l_1-l_2. Thus, as expected, the interference pattern measured is equivalent to the obtained from a classical Hi-Bi FLM with a fiber length $l_v = l_1$-l_2. Note that the performance of this all-PM FLM is similar to a simple Hi-Bi FLM without the need of controlling the polarization state in the fiber loop.

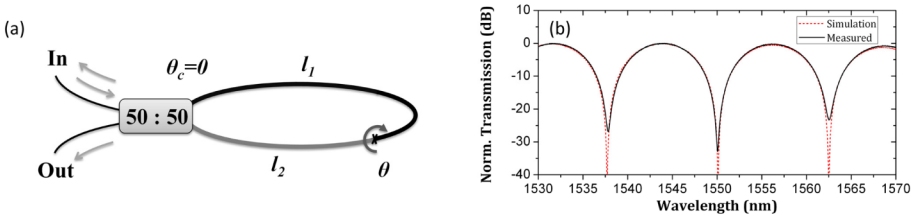

Fig. 1. (a) Schematic of the all polarization maintaining FLM. (b) Simulated and measured transmission spectra of the proposed all-PM fiber loop mirror.

2.2 Three-section all-PM Hi-Bi FLM

However, referring to sensing applications, the previous setup is limited to employ the Hi-Bi fiber of the PM-coupler as the sensing fiber. As a consequence, other types of PM fiber cannot be directly interrogated. This implies that due to the crosstalk between measurands, axial strain and temperature cannot be individually monitored. To overcome this limitation, another polarization-independent FLM setup is presented. In this case, a Hi-Bi fiber section of a different type is inserted inside the fiber loop as depicted in Fig. 2(a). In this case, the FLM behavior becomes more complicated since three Hi-Bi fiber sections are present in the fiber loop. As reported in [11] by the authors and also probed in the first setup, depending on the rotation angle θ between two fiber sections, they can act as a virtual single section of length l_1 + l_2 (θ = 0° + 180k) or l_1-l_2 (θ = 90° + 180k). Taking this into account, if the angles between fibers are appropriately set, the transmission pattern can be simplified to a two-section scheme formed by a Hi-Bi fiber section l_3 and a virtual section $l_v = l_1$-l_2. It is clear that to achieve a virtual section $l_v = l_1$-l_2 the relative angle between them must be $\theta_1 + \theta_2$ = 90° + 180k. Additionally, the rotation angle between $l_1 \rightarrow l_2$ and $l_3 \rightarrow l_2$ must be $[\theta_1, \theta_2] \neq 0° + 90k$ to properly isolate the l_3 contribution.

#249263 Received 1 Sep 2015; revised 28 Oct 2015; accepted 16 Nov 2015; published 19 Nov 2015

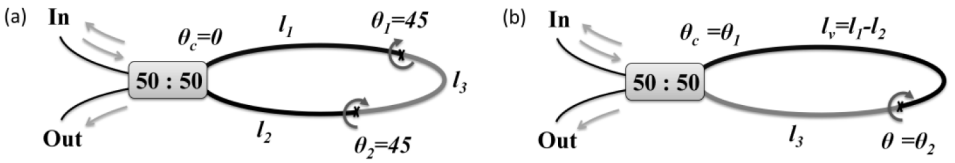

Fig. 2. (a) Experimental and (b) equivalent scheme of the three-section all-PM FLM.

Therefore, considering these two conditions, a three-section polarization-independent Hi-Bi FLM can be formed with a transfer function composed by the contributions of l_3 and l_v. It must be noted that the order of the sections in the loop does not affect the transfer function. Only lengths and relative angles between fibers and the coupler are determinant. Consequently, to simplify the comprehension of the system, the FLM can be understood also as a two-section Hi-Bi FLM with a rotation angle $\theta' = \theta_2$ and $\theta_c' = \theta_1$ as depicted in Fig. 2(b). In accordance, the transfer function of the three-section all-PM Hi-Bi FLM is as follows:

$$T = [\cos((\beta_1 - \beta_2) + \beta_3)\cos(\theta_2)\sin(\theta_1) + \cos((\beta_1 - \beta_2) - \beta_3)\sin(\theta_2)\cos(\theta_1)]^2$$
$$\theta_1 + \theta_2 = 90° + 180k \quad \text{and} \quad [\theta_1, \theta_2] \neq 0° + 90k \tag{4}$$

To validate the proposed scheme, an experimental study was carried out. In the same manner as in the first setup, the output ports of a PM optical coupler with a Hi-Bi fiber (PANDA SM15-PS-U25A; L_B 3.98 mm) were fused to a Hi-Bi all-silica micro-structured fiber (PM-1550–01 NKT Photonics; L_B = 1.75 mm). The length of the PANDA sections were l_1 = 0.50 m and l_2 = 1.04 m and the length of the pure-silica fiber was 2.56 m. Based on Eq. (4), the rotation angles between fibers were set $\theta_1 = \theta_2 = 45°$ to maximize the contributions given by $l_v = l_1$-l_2 and l_3. It is worth noting that $\theta_1 = \theta_2 = 45°$ are fixed so the system is polarization-independent [Eq. (4)]. The system, depicted in Fig. 2(a), was monitored in transmission with a commercial fiber Bragg grating sensors interrogator (Smartec SM125) with a resolution of 5 pm. The experimental and simulated optical spectra can be seen in Fig. 3(a). In addition, the FFT is computed by Matlab software that acquires the optical spectrum, provided by the commercial interrogator, with a scan frequency of 1 Hz. With this technique, the contributions of the different fiber sections can be easily identified at their particular spatial frequencies defined by $Sf(l_n) = l_n/\lambda\ L_{Bn}$. The amplitude of the FFT obtained from the experimental results and the simulation can be seen in Fig. 3(b). It is clear that the contributions from the section l_3 and l_v can be identified at $Sf(l_v)$ = 0.0875 nm^{-1} and $Sf(l_3)$ = 0.95 nm^{-1} (they can also be noted the contributions l_3- l_v and l_3 + l_v.). Additionally, some other contributions are present only in the experimental setup due to the non-ideality of the elements and possible small mismatches in the rotation angles.

3. Sensor validation

3.1 Two-section all-PM Hi-Bi FLM temperature sensor

In order to study the performance improvement of the all-PM Hi-Bi FLMs, a series of experiments were carried out. In these tests, two main aspects were compared. Firstly, the behavior of the proposed two-section all-PM FLM versus the simple Hi-Bi FLM. Secondly, the results using the classical monitoring technique (monitoring the wavelength shift of a valley in the spectrum) were compared to the obtained using the FFT analysis as in [11]. As mentioned previously, the sensing information of the Hi-Bi fiber is encoded in the phase shift $\Delta\phi_n$. Consequently, temperature and strain variations in the fiber will be reflected in a phase change of the FFT at the spatial frequency $Sf(l_n)$. Initially, the sensitivity of the two-section all-PM FLM was measured, using both the classical and the FFT technique, obtaining linear responses of −1.98 nm/°C, and 0.3065 π rad/°C respectively. In the same way, the response to temperature of a simple FLM (formed by a 50:50 SMF optical coupler, a polarization controller and 0.5 m of PANDA fiber) using the FFT analysis was measured as 0.3043 π

#249263 Received 1 Sep 2015; revised 28 Oct 2015; accepted 16 Nov 2015; published 19 Nov 2015

rad/°C. Afterwards, the temperature variation with time was tested for 95 minutes. The results given by a reference probe, with a resolution of 0.01°C, are shown in Fig. 3(c). The temperature measured by the two-section all-PM FLM using the classical method is presented in Fig. 3(d), showing an error over 0.1°C. Figure 3(e) presents the temperature shift measured by the proposed two-section all-PM FLM, monitored using the FFT analysis this time, showing an uncertainty around $5.6 \cdot 10^{-4}$ °C. Finally, the temperature shift measured by a simple Hi-Bi FLM using the FFT technique can be seen in Fig. 3(f). All the temperatures were calculated using the initially measured sensitivities. In the last case, apart from a high number of instabilities, there is a clear mismatch between the reference probe and the reading. This is due to the different temperature trend in the sensing fiber with respect to the single mode fiber of the polarization controller. Two main conclusions can be derived from this experiment. Firstly, the all-PM FLM has a better performance compared to the simple FLM, with an increased stability and more accurate tracking of the temperature. Lastly, it is important to highlight that the proposed FFT monitoring technique provides a resolution over 100 times greater when compared to the classical method using the same optical interrogator.

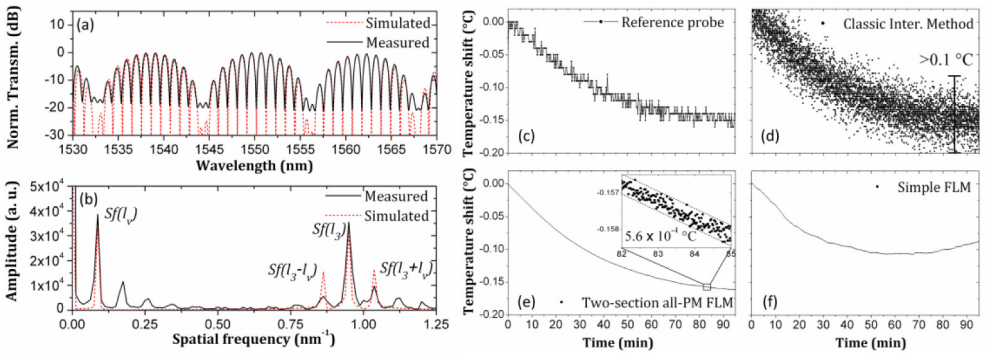

Fig. 3. Experimental and simulated results of the three-section all-PM FLM with an all-silica section: (a) optical spectrum and (b) FFT amplitude. Temperature shift measured by (c) a reference probe, (d) the two-section all-PM FLM using the classical method, (e) the two-section all-PM FLM using the FFT method and (f) a simple Hi-Bi FLM using the FFT analysis.

3.2 Three-section all-PM Hi-Bi FLM strain and temperature sensor

In the second set of experiments, the three-section all-PM FLM [Fig. 2(a)] was validated as a sensor system. The scheme can be understood as a sensor multiplexing scheme with two sensing fibers: PANDA fiber with length l_v and Hi-Bi pure silica section with length l_3. Due to the single material characteristic, the pure silica fiber is insensitive to temperature; thus the strain information can be directly obtained, while the temperature value can be extracted from the PANDA fiber. Other fiber configurations can be used, even using sections of the same PANDA fiber, since the strain information could be obtained from subtracting the temperature value collected from the other fiber section. In either case, it is required to isolate the contributions generated by the two fibers. In this case, only the FFT method was used since it is required to isolate the contributions of the PANDA and the all-silica fiber; $Sf(l_v)$ and $Sf(l_3)$ respectively in Fig. 3(b). In this manner, the phase of the FFT at those spatial frequencies was monitored for strain and temperature variations.

Initially, the sensitivity of the system to temperature was investigated by placing the FLM inside a climatic chamber and performing a temperature sweep from 30 to 65°C. A sensitivity of 0.2782 π rad/°C was measured for the PANDA fiber with a factor $R^2 = 0.99998$. To demonstrate the temperature insensitivity and the crosstalk-free operation of the pure-silica fiber, the raw data of the temperature characterization is presented in Fig. 4(a). It can be observed that the PANDA phase shift $\Delta\phi_v$ matches perfectly with the reading given by the reference probe. It can also be noted as expected, the negligible phase variation $\Delta\phi_3$ of the pure silica fiber. An axial-strain test was also performed to the pure-silica fiber by fixing a

#249263 Received 1 Sep 2015; revised 28 Oct 2015; accepted 16 Nov 2015; published 19 Nov 2015

segment of 15 cm to a translation stage with a minimum step of 17 nm. The test consisted of 260 samples every 12 με and the results can be seen in Fig. 4(b). The sensitivity of the pure-silica fiber to strain was measured as –0.128 π rad/mε with a $R^2 = 0.99956$. The crosstalk-free operation is verified as well, since the phase shift related to the PANDA fiber remained stable. Finally, a study for small temperature variations in a partially-isolated environment was performed. Figure 4(c) shows the results obtained, with an error around $6.2 \cdot 10^{-4}$ °C. Consequently, the sensing error is equivalent to the two-section all-PM FLM. However it has the advantage of having two sensing fibers for two different measurands multiplexed. As a note, simple averaging techniques could considerably increase the resolution.

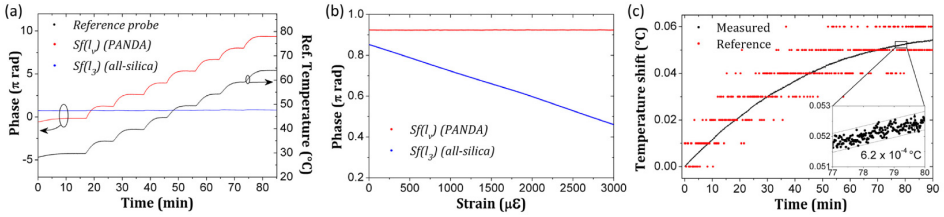

Fig. 4. Phase evolution of the main spatial frequency contributions during (a) the temperature and (b) strain tests. (c) High-resolution temperature measured experimentally.

4. Conclusions

In conclusion, two polarization-independent Hi-Bi fiber loop mirrors have been presented and validated both theoretically and experimentally without the need of polarization controllers. This overcomes one of the main practical limitations of FLMs, which is their high polarization dependence on external perturbations. The first setup is studied under the two-section FLM theory and is based on a PM-optical coupler, whose output ports are fused with a rotation angle of 90° between them. This angle maximizes the interference created, obtaining a simplified transfer function of a simple Hi-Bi FLM, without the dependence on the polarization angles at the ports of the coupler. Another all-PM FLM scheme has also been proposed, with the aim of including a different type of PM sensing fiber inside the loop. In this case, the system behaves as a two-section FLM (with lengths $l_v = l_1 - l_2$ and l_3) if the fibers are fused with the appropriate rotation angles between them. Both systems has been studied, simulated and experimentally tested for ultra-high strain and temperature resolution sensing applications, measuring temperature resolutions of $6 \cdot 10^{-4}$ °C without averaging. In this regard, a comparison between the proposed all-PM FLM and a simple FLM has been performed, showing its superior performance, since the all-PM FLM is not affected by random variations in the polarization states along the SMF. It has been also demonstrated the capability of the system for performing simultaneous temperature and strain measurements without crosstalk.

This study remarkably increases the practical applicability of FLMs because the proposed systems keep the polarization states fixed along the whole loop. Without SMF sections, no polarization controllers are required in the setup. As far as the authors know, this is the first time that such systems are presented and validated. In this manner this study overcomes, together with the FFT monitoring technique, two of the main drawbacks of interferometric FLM sensors to be reliably used in sensing applications; especially when compared to fiber Bragg gratings. That is its multiplexing capability and the high sensitivity to polarization perturbations. Apart from the sensing field, the increase in reliability and robustness of the all-PM FLMs can be exploited in other fields such as fiber lasers, optical filters or optical communications.

Acknowledgments

This work was supported by the Spanish Government project TEC2013-47264-C2-2-R and the FEDER funds.

#249263 Received 1 Sep 2015; revised 28 Oct 2015; accepted 16 Nov 2015; published 19 Nov 2015